

## Article

# Analysis of the Heating Process of Hydraulic Motors during Start-Up in Thermal Shock Conditions

Ryszard Jasiński Faculty of Mechanical Engineering and Ship Technology, Gdańsk University of Technology,  
80-223 Gdańsk, Poland; ryszard.jasinski@pg.edu.pl

**Abstract:** Conditions that prevail during harsh winters and hot summers pose a serious challenge for machine designers building devices suitable for operation in extreme weather. It is essential for the designers and the users to define the principles and conditions for the safe operation of machines and devices with hydraulic drive in low ambient temperatures. Bearing in mind the above, the author tested the hydraulic motors in thermal shock conditions (cold motors were fed with a hot working medium). This enterprise required the design and construction of a specialized stand for testing hydraulic motors, including satellite motors, in thermal shock conditions. The stand was equipped with the apparatus and a system for measuring the temperature of the moving parts of the satellite motor. The experimental tests were conducted in the laboratory of the Faculty of Mechanical Engineering and Ship Technology at Gdańsk University of Technology. The paper presents the results of tests of a correctly and incorrectly operating satellite motor during start-up in thermal shock conditions. The results concerned the course of oil temperatures, temperatures of heated elements, oil pressures, and the pressure drop in the motor. The influence of the oil pressure drop in the motor on its temperature increase was determined. The distributions of the temperature fields of the heated elements of the satellite motor during start-up in thermal shock conditions were derived by means of computer simulation. The utilization of the distribution of the temperature fields of the motor elements enables the evaluation and analysis of the work of this unit. The conducted tests may determine the conditions for the proper operation of hydraulic motors started in thermal shock conditions.

**Keywords:** hydraulic motor; thermal shock conditions; hydraulic motor; low ambient temperature; energy balance; computer simulation; power losses



**Citation:** Jasiński, R. Analysis of the Heating Process of Hydraulic Motors during Start-Up in Thermal Shock Conditions. *Energies* **2022**, *15*, 55. <https://doi.org/10.3390/en15010055>

Academic Editors: Helena M. Ramos, Marian Janusz Łopatka, Arkadiusz Rubiec and Piotr Patrosz

Received: 11 November 2021

Accepted: 19 December 2021

Published: 22 December 2021

**Publisher's Note:** MDPI stays neutral with regard to jurisdictional claims in published maps and institutional affiliations.



**Copyright:** © 2021 by the author. Licensee MDPI, Basel, Switzerland. This article is an open access article distributed under the terms and conditions of the Creative Commons Attribution (CC BY) license (<https://creativecommons.org/licenses/by/4.0/>).

## 1. Introduction

Hydraulic systems that are used in many machines and devices operated in a given climatic zone should work without failure in various weather conditions characteristic for this zone. The influence of low temperature on the hydraulic drive's ability to work during the machine start-up period, especially after a long period of inactivity, is extremely unfavorable.

Start-up of hydraulic motors at low ambient temperatures can be performed with the use of cold or hot working medium, most often in the form of hydraulic oil [1–4].

The author has been researching hydraulic components (pumps, valves, motors) at low ambient temperatures for many years. When analyzing the starting conditions of hydraulic systems (hydraulic motors) at low ambient temperature, two cases of supplying a cooled motor with cold or warm working fluid can be distinguished [2–4].

In the first case, the entire hydraulic system, including the oil, is at the ambient temperature during start-up.

In the second case, just before starting the system, the oil is heated in the hydraulic system to a temperature that is significantly higher than the low ambient and motor temperature (thermal shock conditions).

The author decided to conduct experimental tests on several designs of hydraulic motors (orbital motors, satellite motors, piston motors) operating at low ambient temperatures

in order to evaluate the operation of motors and hydraulic systems in these conditions [3]. These tests were aimed at facilitating the measurement of changes in the temperature of cooperating elements of hydraulic motors during start-up in thermal shock conditions.

Based on the requirements of the Polish Standard [5] and the Polish Register of Shipping (PRS) [6,7] regarding the ability to operate hydraulic motors in negative temperature conditions, in special cases of supplying a hot working medium to a cold unit, e.g., ship's deck equipment, the temperature difference between assembly and working medium can reach even 80 K.

In [8], the usefulness of the thermodynamic method for the measurement of motor efficiency has also been discussed. Measuring instruments that directly indicate the overall efficiency were developed on the basis of this method. Tests and research of satellite motors [8] conducted previously served as the basis for detailed tests and research of the motors in thermal shock conditions conducted by the author of this article. The authors of [9] focused on examining, among others, the ability of a displacement motor to start at low temperatures. The problems of operation of hydrostatic drive and control systems in working machines in the winter are presented in [10]. The tests of the gear pumps at low ambient temperatures are described in [11]. In the paper [12], the authors provide an evaluation of the electro-hydraulic system and a discussion on the usage of hydraulic oil by non-road mobile working machines in sub-zero conditions. Article [13] presents the impact of temperature changes on fluid properties, especially viscosity, density, and bulk modulus. It also describes how these changes in fluid properties affect the operation of piston pumps. The publication [14] presents selected problems regarding the influence of the lowered temperature on the properties of construction materials and working fluids as well as the influence of temperature on the phenomena occurring in hydraulic drives and control systems.

Hydraulic pumps and hydraulic motors [15–17] are the basic hydraulic system components vulnerable to energy losses. The issues of energy losses in hydraulic components and systems were discussed in papers [18,19]. Volumetric, pressure, and mechanical losses are determined for a given hydraulic device operating in steady conditions, disregarding the effect of heat transfer in such a device, since it can be considered insignificant in the total balance of energy losses [20–23]. A proposal to reduce energy consumption in a hydraulic system is presented in paper [24]. In the process of starting a hydraulic machine, the heat exchange on the path whose waypoints include working fluid—elements of hydraulic components—the environment, greatly impacts the efficiency of energy conversion in these components of devices, especially during the start-up of cold components (motors) supplied with hot working fluid, which was proved in [1–4,25–27].

The issues of heat transfer during the start-up of a hydraulic motor have been described in publications including [28–30], while numerical methods of calculating temperature fields are presented in the book [31].

The start-up of a cooled hydraulic motor powered by a working medium of a higher temperature will result in a transient heat transfer  $\dot{\Phi}_\alpha$  from the oil to the motor components. The motor and oil temperatures will taper to the new set values (Figure 1). During this time, the motor will absorb an appropriate amount of heat, assuming a new value of the internal energy level.

As the temperature of the flowing fluid is higher than the temperature of the motor elements, a laminar boundary layer is formed along the flow path at the surface of the motor elements in which the fluid particles move parallel to the walls (Figure 1). Even in the case of a turbulent flow, a laminar layer is formed in direct vicinity of the wall. In this layer, the heat flow from the oil to the motor elements proceeds only through conduction (moreover, this layer can be penetrated by radiation) [32].

The article presents a description of the heating processes of unloaded hydraulic motors.

Currently, the influence of thermal shock conditions on the performance of hydraulic (satellite) motors is not widely known. It is important for designers and users to define the principles and conditions of safe operation of machines and devices with hydraulic

drives operated in low ambient temperatures. The article presents a model of the heating process of the elements of a hydraulic motor (also a satellite motor) during start-up in thermal shock conditions. A newly developed method of testing hydraulic motors in thermal shock conditions has also been presented. This method required designing and constructing a novel and specialized stand for testing hydraulic motors, including satellite motors, in thermal shock conditions. The stand was equipped with the apparatus and system for measuring the temperature of both fixed and moving parts of the satellite motor. On the basis of the experimental tests of the motor in thermal shock conditions, a method for determining the correct or incorrect operation of the motor has been developed. The computer simulation method makes it possible to analyze the heating process of hydraulic components as shown in the article on the basis of a satellite motor. Due to a good correlation between experimental and computer simulation results, it is justified to use simulations for calculation of the heating process of other hydraulic motors.

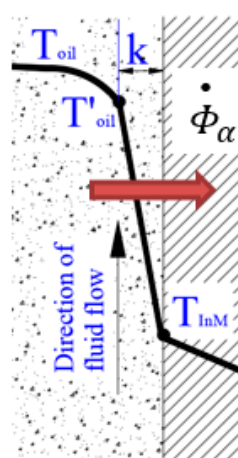


**Figure 1.** Fluid temperature distribution at the surface of the motor element, where  $k$ —thickness of the laminar boundary layer,  $T_{oil}$ —temperature of the flowing oil,  $T'_{oil}$ —oil temperature at the border of the boundary layer,  $T_{InM}$ —temperature of the internal surface of the motor body.

In Section 2, a model of the heating process of the elements of a hydraulic motor during start-up in thermal shock conditions is presented. Additionally, a model of heating a cold satellite motor by a flowing hot fluid is presented and described. Section 3 shows the influence of frictional heat in the motor on the increase in oil temperature. The significance of the oil pressure drop in the unloaded motor on the increase in its temperature is determined. A description of a specialized stand for testing hydraulic motors, including satellite motors, in thermal shock conditions is provided in Section 4. The stand was equipped with apparatus and a system for measuring the temperature of the moving parts of the satellite motor. Identification of the satellite motor parameters for correct operation is contained in Section 5. Numerous tests of the motor in thermal shock conditions enabled the creation of parameter areas (including temperature difference between the working medium and the motor at the initial moment, and the rotational speed), at which the motor operated correctly or incorrectly. Section 6 presents the test results for the satellite motor for three cases, i.e., for the motor working correctly, incorrectly and temporarily incorrectly. In Section 7, the heating process of the satellite motor elements during start-up in thermal shock conditions with the use of computer simulation is given. Section 8 contains the conclusions that were drawn in the course of work.

## 2. Model of the Heating Process of Hydraulic Motor Elements

Low-speed hydraulic motors are also used in machines and devices with hydraulic drives. For example, orbital or satellite motors are often used in hydraulic systems (Figure 2).

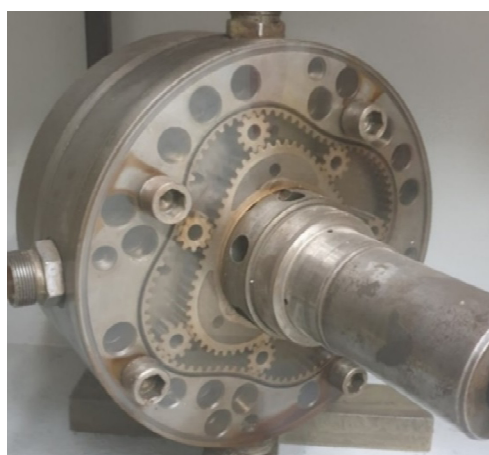


Figure 2. Satellite hydraulic motor by Hydroster.

In order to present the heating process of a hydraulic motor by means of hot oil flowing through the cooled unit, a model of this motor was made (Figure 3). In the model, due to the very small external leakage flow rate, it can be assumed that the oil flow rates at the input  $Q_1$  and output  $Q_2$  are approximately the same:

$$Q_1 - Q_{leaks} \cong Q_2. \tag{1}$$

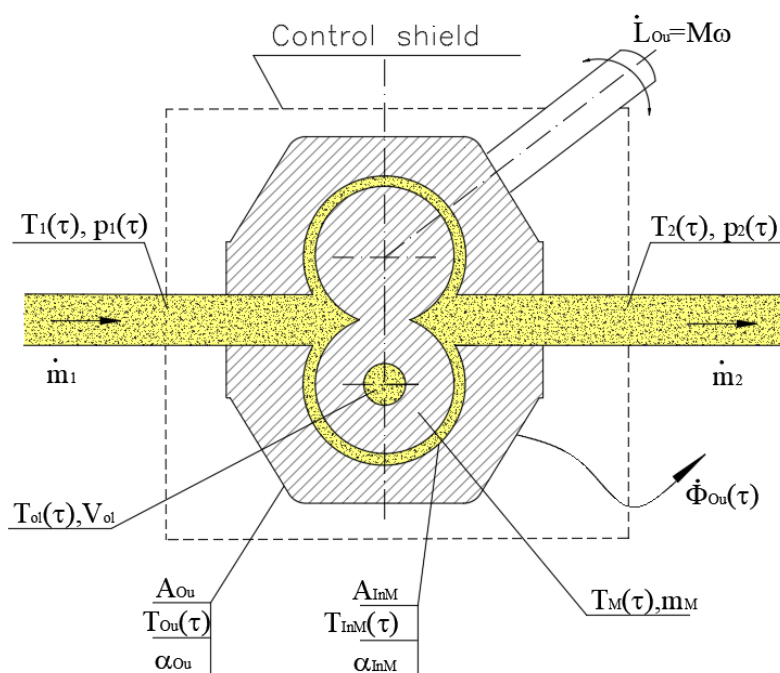


Figure 3. Parameters for determining the energy balance in a hydraulic motor ( $A$ —surface,  $T$ —temperature,  $m$ —mass,  $\alpha$ —heat transfer coefficient,  $p$ —pressure,  $\dot{m}$ —mass flow,  $\dot{\Phi}$ —thermal energy flux; Symbols:  $InM$ —inner surface of motor,  $Ou$ —outer,  $M$ —motor,  $ol$ —fluid (oil), 1—inlet, 2—outlet).

According to the first law of thermodynamics, the energy  $E_1$  supplied to the hydraulic motor during the start-up is the sum of the energy output  $E_2$  and the energy increase  $\Delta E$  of the system:

$$E_1 = E_2 + \Delta E. \tag{2}$$

In elementary time  $d\tau$ , the hydraulic motor exchanges heat  $d\Phi_{Ou}$  with the environment and returns elementary external work  $dL_{Ou}$ . The internal energy of the motor changes by the value of  $dE$ .

Using the balance form of the first law of thermodynamics, the following equation is obtained:

$$dm_1 \left( u_1 + p_1 \cdot v_1 + \frac{w_1^2}{2} + g \cdot h_1 \right) = dE + dL_{Ou} + d\Phi_{Ou} + dm_2 \left( u_2 + p_2 \cdot v_2 + \frac{w_2^2}{2} + g \cdot h_2 \right) \quad (3)$$

where

$u_1, u_2$ —internal energy of the working fluid at the motor input and output;  
 $v_1, v_2$ —specific volume of the working fluid at the motor input and output.

Most often, the cross-sectional areas of the liquid flow in the channels on the inflow and outflow of hydraulic motors and their positions are the same, which translates into equal velocity of the liquid flow  $w$  and height  $h$ . Therefore, the energy balance equation can be simplified by eliminating kinetic and potential energy, because their differences are close to zero.

This simplification is also justified for the liquid flow velocities  $w$  and heights  $h$ , which differ to quite significant limits, which was demonstrated, inter alia, in [8].

Assuming that for the unloaded motor, the external work  $dL_{Ou} = 0$  and mass flows at the input and output  $\dot{m}_1 = \dot{m}_2 = \dot{m}$ , i.e.,  $dm_1 - dm_2 = 0$ , Equation (3) can be written as:

$$\dot{m} \cdot (u_1 + p_1 \cdot v_1) = \dot{E} + \dot{\Phi}_{Ou} + \dot{m} \cdot (u_2 + p_2 \cdot v_2). \quad (4)$$

By introducing the enthalpy according to the definition  $i = u + p \cdot v$  into Equation (4), the following result was obtained:

$$\dot{m} \cdot i_1 = \dot{m} \cdot i_2 + \dot{E} + \dot{\Phi}_{Ou} \quad (5)$$

where

$i_1, i_2$ —enthalpy on input and output from the control shield.

The transformation of Equation (5) yields:

$$\dot{m} \cdot (i_1 - i_2) = \dot{E} + \dot{\Phi}_{Ou}. \quad (6)$$

The difference of the energy flows at the input and output from the motor depends on:

- The flux of energy flowing from the external surface of the motor to the environment  $\dot{\Phi}_{Ou}$ , which is expressed by the equation:

$$\dot{\Phi}_{Ou} = \alpha_{Ou} \cdot A_{Ou} \cdot (T_{Ou} - T_{ot}) \quad (7)$$

where

$\alpha_{Ou}$ —average heat transfer coefficient to the environment from the external surface of the motor  $A_{Ou}$ ;

$T_{Ou}$ —average temperature of the outer surface of the motor;

$T_{ot}$ —ambient temperature.

- The flux of thermal energy increasing the internal energy of the oil in the motor and motor elements:

$$\dot{E} = \dot{E}_{ol} + \dot{E}_M. \quad (8)$$

$\dot{E}_{ol}$ —the flux of thermal energy increasing the internal energy of the oil in the motor:

$$\dot{E}_{ol} = V_{ol} \cdot \rho_{ol} \cdot c_{ol} \cdot \frac{dT_{ol}}{d\tau} \quad (9)$$

where

$V_{ol}$ —volume of the chambers and channels of the motor;

$\rho_{ol}$ —oil density;

$c_{ol}$ —specific heat of oil;

$T_{ol}$ —oil temperature.

$\dot{E}_M$ —the flux of thermal energy increasing the internal energy of the motor:

$$\dot{E}_M = \sum_{j=1}^n m_j \cdot c_j \cdot \frac{dT_j}{d\tau} \quad (10)$$

where

$m_j$ —the mass of  $j$ -th motor element;

$c_j$ —specific heat of material of  $j$ -th element;

$T_j$ —average temperature of  $j$ -th motor element.

The flux of thermal energy flowing from the oil to the motor is equal to:

$$\dot{\Phi}_\alpha = A_{InM} \cdot \alpha_{InM} \cdot (T_{ol} - T_{InM}) \quad (11)$$

where

$A_{InM}$ —heat exchange surface between the flowing oil and the motor;

$\alpha_{InM}$ —heat transfer coefficient from oil to motor;

$T_{ol}$ —average oil temperature;

$T_{InM}$ —the average temperature of the heat transfer surface between the flowing oil and the motor.

The flux of thermal energy flowing from the oil to the internal surface of the motor is equal to the flux of thermal energy increasing the internal energy of the motor elements and the flux of thermal energy flowing from the external surface of the motor to the environment:

$$\dot{\Phi}_\alpha = \dot{E}_M + \dot{\Phi}_{Ou}. \quad (12)$$

A hydraulic motor consists of two groups of elements: movable and fixed. The simplified diagram of a motor (Figure 4) shows the flow of energy streams.

The flux of thermal energy flowing from the oil  $\dot{\Phi}_\alpha$  to the movable parts  $\dot{\Phi}_B$  and fixed parts  $\dot{\Phi}_S$  of the motor is equal to:

$$\dot{\Phi}_\alpha = \dot{\Phi}_B + \dot{\Phi}_S \quad (13)$$

$$\dot{\Phi}_\alpha = A_{InB} \cdot \alpha_{InB} \cdot (T_{ol} - T_{InB}) + A_{InS} \cdot \alpha_{InS} \cdot (T_{ol} - T_{InS}) \quad (14)$$

where

$B$ —index denoting a movable element;

$S$ —index denoting a fixed element.

A satellite hydraulic motor consists mainly of fixed elements: body, covers, and supply manifold, while its movable elements include the rotor and satellites (Figure 5). Due to the fact that the fixed elements are connected to each other, they are treated as a whole and create a single fixed element.



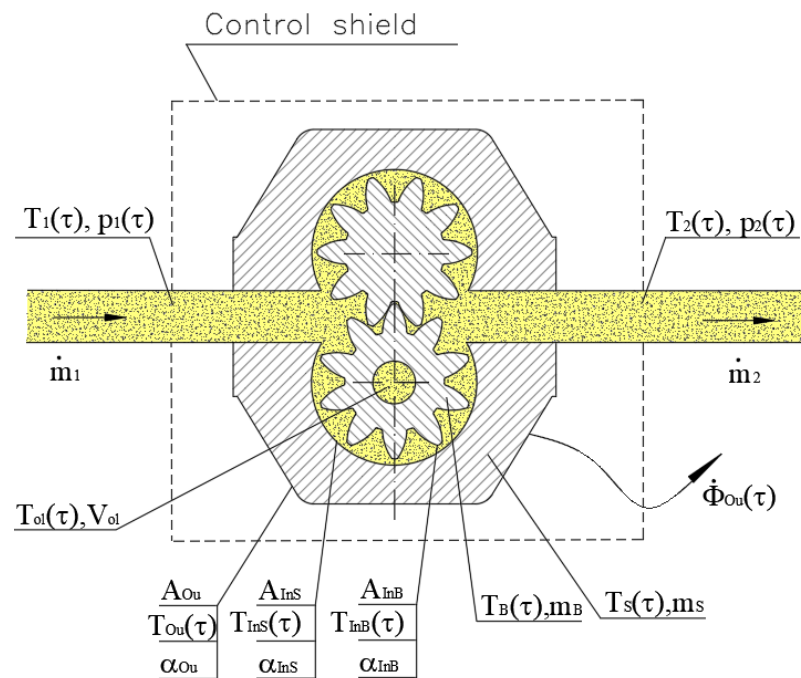


Figure 4. Model of heating of a cooled hydraulic motor by flowing hot fluid (division into movable (B) and fixed (S) motor parts); all denotations are the same as in Figure 3 above.

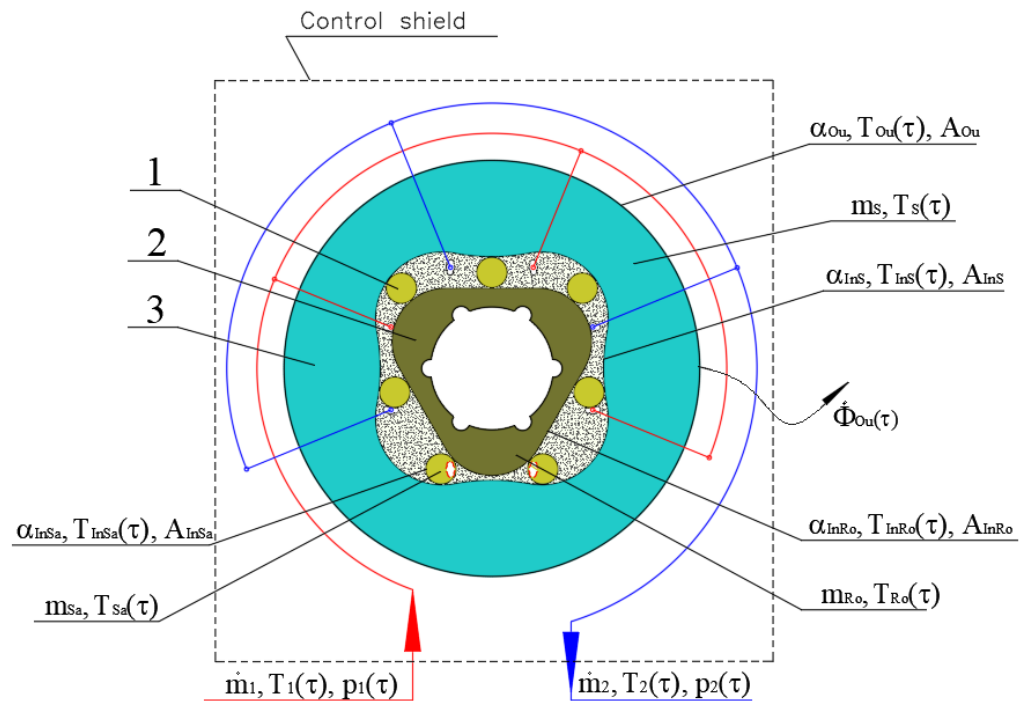


Figure 5. Model of heating of a cooled motor by flowing hot fluid (on the example of a satellite motor); 1—satellite, 2—rotor, 3—fixed elements.

On the other hand, movable elements, such as the satellites and rotor, will be treated as the elements that are heating independently.

In a satellite hydraulic motor (Figure 5), the thermal energy flux that flows from oil  $\dot{\Phi}_\alpha$  to satellites  $\dot{\Phi}_{Sa}$ , rotor  $\dot{\Phi}_{Ro}$ , and fixed parts  $\dot{\Phi}_S$  of the motor is equal to:

$$\dot{\Phi}_\alpha = \dot{\Phi}_{Sa} + \dot{\Phi}_{Ro} + \dot{\Phi}_S \tag{15}$$

$$\dot{\Phi}_\alpha = A_{InSa} \cdot \alpha_{InSa} \cdot (T_{ol} - T_{InSa}) + A_{InRo} \cdot \alpha_{InRo} \cdot (T_{ol} - T_{InRo}) + A_{InS} \cdot \alpha_{InS} \cdot (T_{ol} - T_{InS}) \quad (16)$$

where

*Ro*—index denoting rotor;

*Sa*—index denoting satellite;

*S*—index denoting fixed elements.

### 3. The Influence of Frictional Heat in a Motor on the Increase in the Oil Temperature

In an unloaded motor, the entire power loss occurring in the motor ( $Q \cdot \Delta p_{12}$ ) is converted into a frictional heat energy flux.

For example, in an unloaded SOK 100 [16] motor operating at a rotational speed of 250 rpm, powered by oil at 43 °C, the pressure drop was about 1.3 MPa [33].

Therefore, it is assumed that the entire friction heat flux will be absorbed by the oil, which will increase its internal energy (temperature), and then, the flux can be transferred to the motor elements through convection. In order to determine the extent of the oil temperature change due to the frictional heat in the motor, an analysis presented below was applied.

The energy balance of the oil flow through the channels of an unloaded motor (Figure 6) can be compared to the energy balance of the oil flowing through a throttle valve [8]. The adiabatic flow of the oil through the throttle valve is accompanied by equal enthalpy at the inlet and the outlet of the valve  $i_1 = i_2$  (Figure 7).

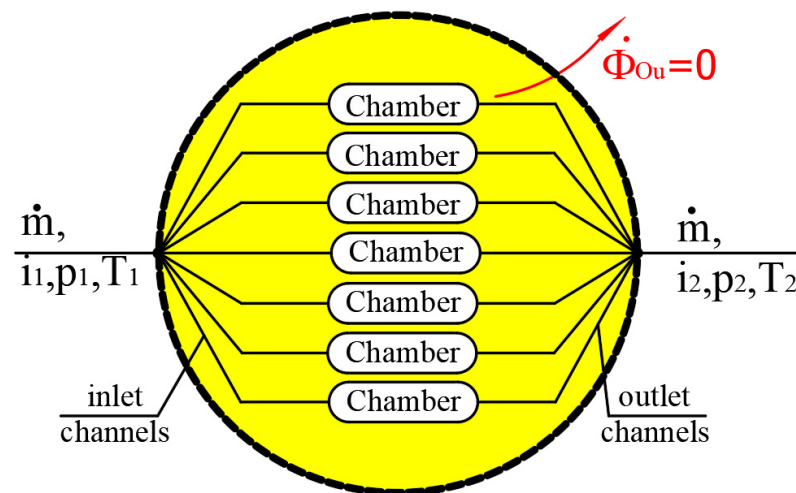


**Figure 6.** Parameters of the working liquid at the inlet and the outlet of an unloaded hydraulic motor (enthalpy equality occurs  $i_1 = i_2$ ).

Isenthalpic oil temperature increase  $\Delta T_i$  is a superposition of the temperature increase  $\Delta T_{fmax} = T_{2i} - T_{2s}$  proportional to the energy losses in the motor (throttle valve) and the increase  $\Delta T_{sE} = T_{2s} - T_1 < 0$  accompanying the adiabatic—isentropic expansion of the liquid [8]:

$$\Delta T_i = \Delta T_{fmax} + \Delta T_{sE}. \quad (17)$$

The finite value of the pressure increase  $\Delta p_{21}$ , for the initial temperature  $T_i$  of the medium, corresponds to the temperature increase by the value of:

$$\Delta T_i = \bar{\delta}_i \cdot \Delta p_{21} \quad (18)$$

where

$\bar{\delta}_i$ —proportionality factor [8].



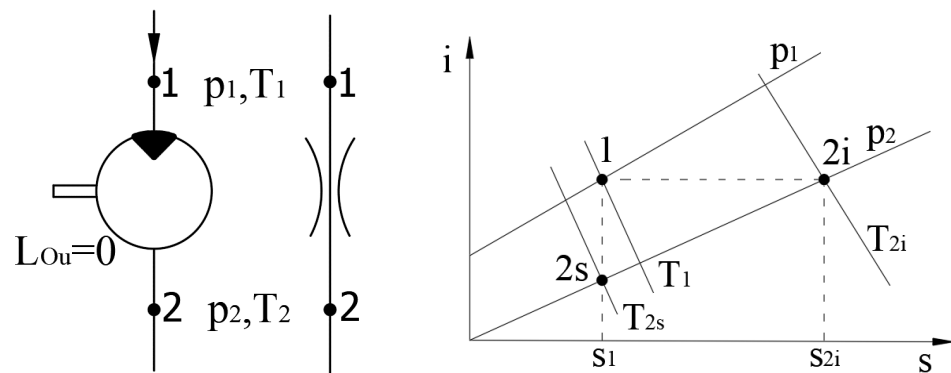


**Figure 7.** Increase in liquid temperature in the unloaded motor model ( $T$ —temperature,  $p$ —pressure,  $L_{Ou}$ —external work,  $i$ —specific enthalpy of the working fluid,  $s$ —specific entropy of the working fluid,  $T_{2i}$ —end temperature of the isenthalpic transformation,  $T_{2s}$ —end temperature of the isentropic transformation; symbols: 1—inlet, 2—outlet).

Equation (17) can be used to determine the temperature rise  $\Delta T_{fmax}$ . After the transformation [8], the following equation was obtained:

$$\Delta T_{fmax} = \Delta T_i - \Delta T_{sE} = \bar{\delta}_f \cdot \Delta p_{21} \quad (19)$$

where

$\bar{\delta}_f$ —proportionality factor [8].

On the basis of the presented analysis of the impact of the pressure drop in the hydraulic motor, it can be concluded that for the pressure drop of 1.3 MPa [33], the liquid temperature will increase by about 0.6 °C (Figure 8).

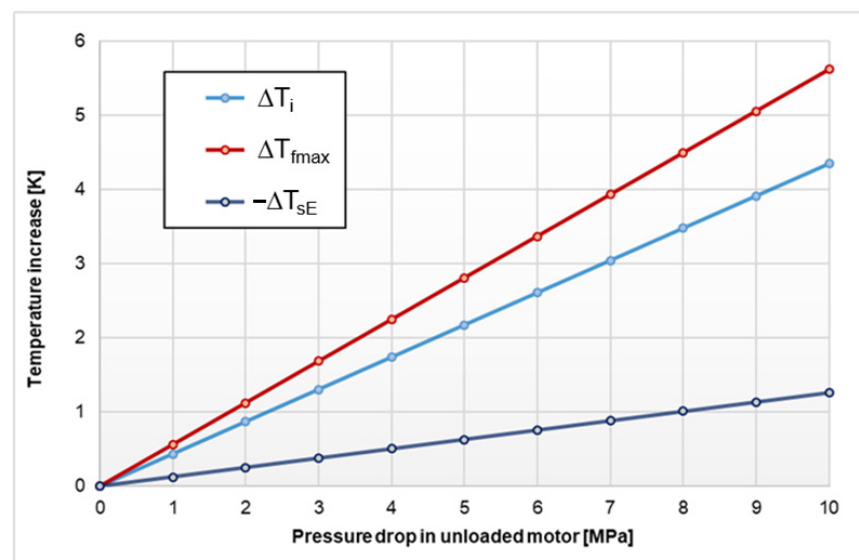


**Figure 8.** Isenthalpic temperature increase  $\Delta T_i$  and increase in  $\Delta T_{fmax}$  are proportional to the loss of hydraulic energy in the unloaded motor (throttle valve) depending on the pressure drop for the Hydrol 40 mineral oil at the temperature of 40 °C at the inlet.

#### 4. The Object of Research and the Test Stand

An M1 satellite motor with a displacement of 0.4 dm<sup>3</sup>/rev was used for the tests. The basic technical data specified by the manufacturer of this motor are as follows: rotational speed in the range from 0 to 160 rpm, maximum rotational speed of 250 rpm, nominal pressure  $p_n = 16$  MPa, and maximum pressure  $p_{max} = 25$  MPa.



In order to obtain the exact temperature distribution of the motor elements operated in thermal shock conditions during the tests, technical documentation including the mounting of the temperature sensors (Figure 9) was prepared.

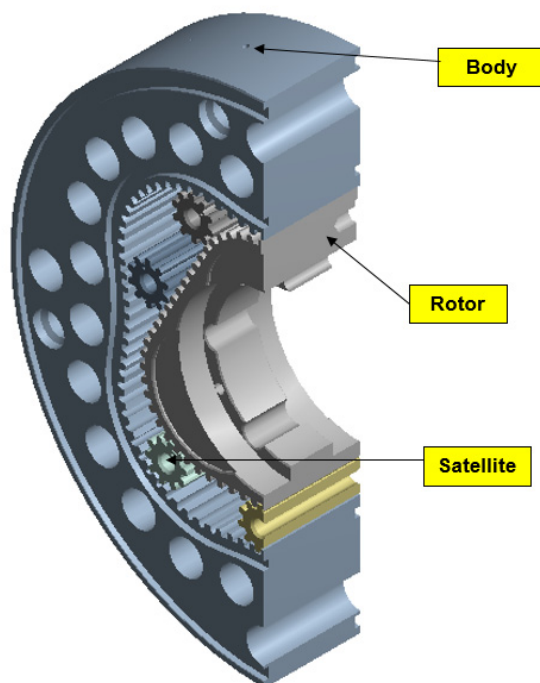


**Figure 9.** Elements of the M1 satellite motor where the temperature sensors were placed. During the experimental tests of the motor, the temperatures of the rotor and fixed elements were measured. The heating of the satellite was conducted in a specially made research system.

The motor for tests in low ambient temperatures was custom-made. It featured holes in the fixed elements for thermoelectric sensors (sheathed type J thermocouple with MT-G socket, thermocouple class: 1, socket operating temperature  $-20$ – $150$  °C) for temperature measurement. Subsequently, the assembly of the motor was carried out. Semiconductor temperature sensors AD 590 produced by Analog Devices were placed in the movable parts of the motor. It required high precision and caution in order to avoid the damage of the sensors and cables leading out through the motor shaft.

There were two sensors placed in the front cover (thermocouple and semiconductor temperature transducer located away from the heat source). They were inserted at the same depth to compare the recorded temperature curves with the thermocouple and semiconductor temperature transducer. The temperatures in the cover near the satellite and rotor cooperation surfaces were also recorded using two thermocouples. There were also two thermocouples placed in the rear cover, one far from the heat source and the other near the heat source. Three thermocouples were placed in the body (far from the heat source, near the heat source, and in the center of the body). Two semiconductor temperature transducers were glued into the rotating rotor.

Temperature sensors made it possible to accurately register temperature changes in the characteristic places. The recorded temperatures made it possible to determine the average temperatures of the motor elements, facilitating the determination of the maximum permissible temperature differences between the motor and the oil, allowing proper operation of the M1 motor.

In order to send the signal from the temperature sensors placed in the rotating rotor to the recorder, signal transmission through a specially made brush-measuring device was used.

The operation principle of the brush device consists in the fact that the signals coming from the semiconductor temperature transducers located in the rotor and the motor shaft

are transmitted through the wires drawn through the shaft to the slip rings placed on the motor shaft extended by a sleeve. The signal from the slip rings is further transmitted by brushes to the data acquisition modules.

Special granules were placed inside the housing of the brush device to absorb the ambient moisture. As a result, when the motor cooled down, no ice layer was formed on the slip rings in the chamber.

The test stand to test hydraulic motors was built in the laboratory of the Faculty of Mechanical Engineering and Ship Technology at Gdańsk University of Technology.

The hydraulic motors were placed in a low-temperature chamber. During the tests of the motor, the temperatures of the movable and fixed elements, the oil temperature at the inlet and the outlet of the motor, oil pressure at the inlet and the outlet, as well as rotational speed and flow rate were measured (Figure 10). The motor was tested with Total Azolla ZS 46 oil.

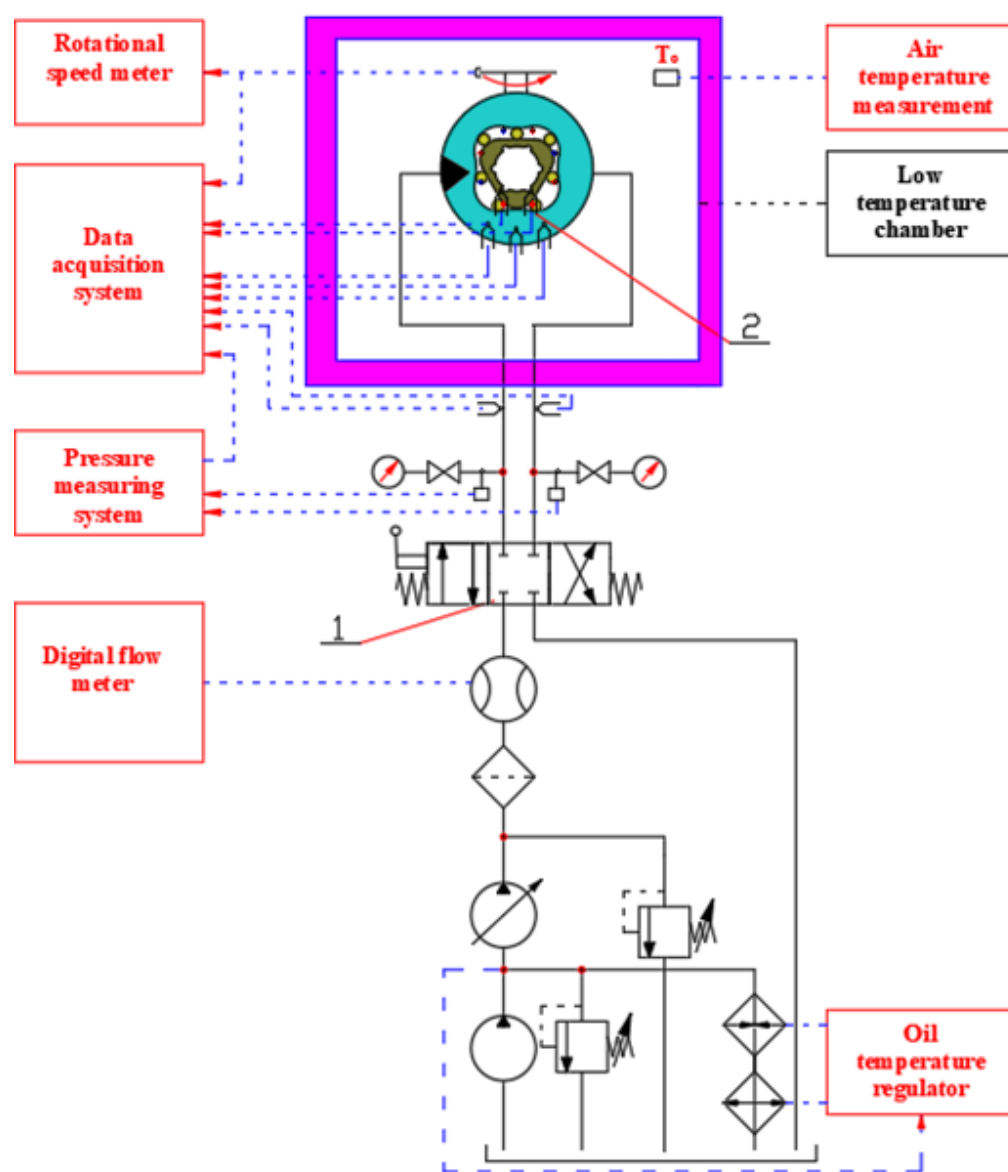


**Figure 10.** Schematic drawing of the hydraulic system with satellite motor (1—spool valve, 2—temperature sensors located in the movable and fixed parts of the motor).

The measurement data generated during the tests of the M1 satellite motor in thermal shock conditions were recorded with the use of fast and accurate electronic systems.

In the measuring system, the measurement data collection device was used to transmit and record the results. The system uses the RS-485 bus to transmit measurement data and commands controlling the operation of individual system modules (ADAM—4000 series modules manufactured by Advantech). Apart from temperature sensors, flow meters and a rotational speed meter were connected to the system. The system controller was a PC equipped with the VisiDaq software package produced by Advantech, which allowed the acquisition, analysis, and presentation of data. During the tests, all the measured values were observed on the computer display monitor in the form of characteristics or digital displays. The data were processed in Excel.

### 5. Identification of the Satellite Motor Parameters for Correct Operation

Tests of the M1 motor start-up in thermal shock conditions were performed at different initial temperatures of the cooled motor and hot oil for different values of the flow rate leap.

The initial parameters were selected in such a way that, for example, for an oil temperature of about 50 °C, a low ambient temperature and the flow rate were set in such a way that a malfunction could occur. If it did not, the ambient temperature was lowered or the value of the flow rate leap was increased.

The following waveforms were obtained: temperatures of the movable and fixed elements of the motor; oil temperature at the inlet and the outlet of the motor; flow rate; shaft rotational speed; oil pressure at the inlet and the outlet of the motor.

The malfunction of the motor during the test was indicated by unstable rotational speed, a sharp increase in the oil pressure at the inlet to the motor, and a pressure drop at the motor outlet.

Numerous tests of the motor in thermal shock conditions enabled the creation of parameter areas (including temperature difference between the working medium and the motor at the initial moment, and the rotational speed), at which the motor operated correctly or incorrectly (Figure 11). The most noticeable symptoms of correct or incorrect operation consisted of the increase in the liquid pressure in the motor inlet channel, decrease in the rotational speed, and increase in the element temperature in excess of the motor supply oil temperature.

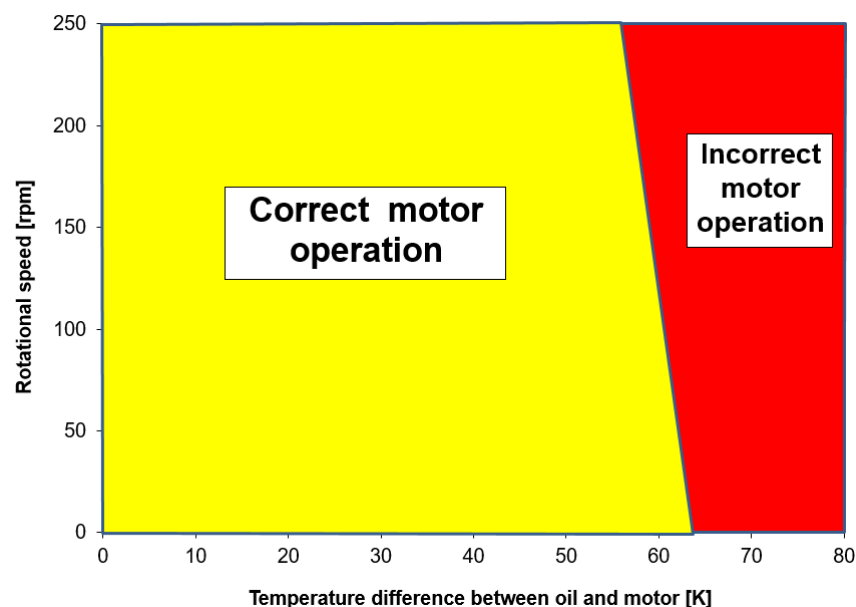


**Figure 11.** The areas of parameters of the correct and incorrect operation of the M1 unloaded motor with 23  $\mu\text{m}$  axial clearance when started in thermal shock conditions.

The satellite hydraulic motor with the displacement of 0.4  $\text{dm}^3/\text{rev}$  started in thermal shock conditions worked correctly as long as the temperature difference between the warm oil and the cooled motor does not exceed 55 K and the rotational speed does not exceed 250

rpm. The lower the shaft revolutions (the lower the flow rate of oil flowing through the motor), the greater the temperature difference at which the motor could operate.

## 6. Results of the Experimental Tests of the Satellite Motor in Thermal Shock Conditions

Dozens of tests of the satellite motor with the displacement of  $0.4 \text{ dm}^3/\text{rev}$  were conducted. The fastest process of heating the motor elements took place at the highest rotational speed (during the highest flow rate).

As an example, specially selected results of three tests of a satellite motor started up in thermal shock conditions for the following cases will be presented:

- The motor was working correctly (temperature difference between hot oil and cold motor 50 K, obtained rotational speed 250 rpm);
- The motor was working incorrectly (temperature difference between hot oil and cold motor 70 K, obtained rotational speed 255 rpm);
- The motor was temporarily working incorrectly (temperature difference between the hot oil and the cold motor 58 K, obtained rotation speed 185 rpm).

In the first of the above-mentioned cases, the test was performed by flooding cold motor whose initial temperature was  $-6 \text{ }^\circ\text{C}$  with oil at the temperature of  $44 \text{ }^\circ\text{C}$ . The resulting rotational speed was 250 rpm. The motor worked correctly in these conditions.

In the recorded waveforms (Figure 12), it can be seen that the oil pressure difference at the inlet and the outlet of the motor from the moment of start-up was initially 2 MPa, and after 50 s, it decreased to about 1 MPa. After this time, the value was constant. The rotational speed and the flow rate remained at the same level from the moment of start-up.

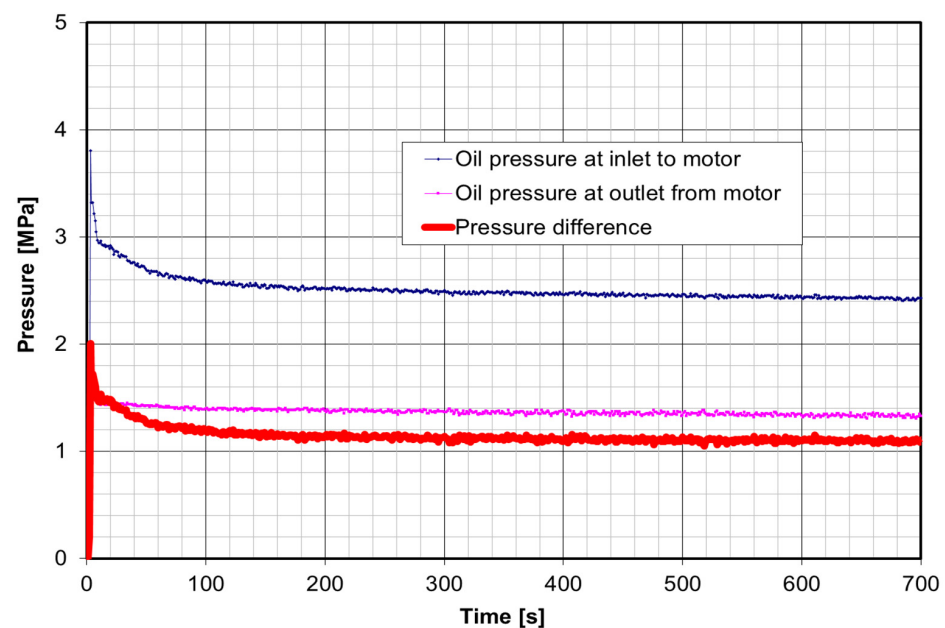


**Figure 12.** Characteristics of the oil pressure at the inlet and the outlet of the motor and the pressure difference as a function of time (ambient temperature (motor)  $-6 \text{ }^\circ\text{C}$ , oil temperature  $44 \text{ }^\circ\text{C}$ , obtained rotational speed approximately 250 rpm).

The effect of the pressure drop in the hydraulic motor in this case was low. The oil temperature increase due to the pressure loss was less than 1 K (Figure 8). The temperature difference between the warm oil and the cold motor was  $50 \text{ }^\circ\text{C}$  initially.

The rotor temperature during 200 s reached almost  $38 \text{ }^\circ\text{C}$  (Figure 13), which meant a very fast heating process. The body warmed up much more slowly, which was mainly due to its large mass in relation to its heat transfer surface area.

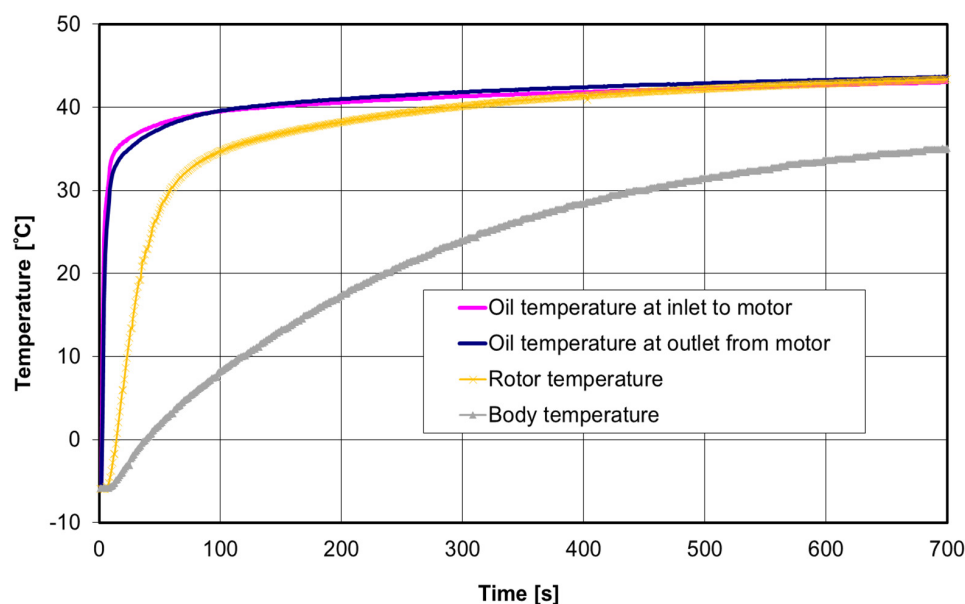


**Figure 13.** Characteristics of the temperatures of rotor, body, and oil at the inlet and the outlet of the motor as a function of time (ambient temperature (motor)  $-6^{\circ}\text{C}$ , obtained rotational speed approximately 250 rpm).

During the second test (b) of the motor in the thermal shock conditions, with the shaft rotating at a speed similar to the previous test, i.e., approximately 255 rpm, symptoms of incorrect motor operation were noted. The initial temperature of the cold motor was  $-20^{\circ}\text{C}$ , while the temperature of the warm oil supplied was  $50^{\circ}\text{C}$ .

Such a large temperature difference between the motor and the oil caused a rapid increase in the temperature of smaller movable elements (satellites). There was a blockage of these elements between the covers and an increase in the friction. There was also a significant increase in the pressure at the inlet to the motor, i.e., a large pressure difference between the inlet and the outlet of the motor, reaching about 7 MPa (Figure 14).

As it can be seen from the presented characteristics, symptoms of the incorrect motor operation, i.e., the increase in the oil pressure at the inlet to the motor to 7.2 MPa (Figure 14) appeared after 18 s. After 160 s from starting the motor, the oil pressure at the entrance to the motor decreased to 2 MPa. The temperature of the motor elements increased faster (Figure 15) than in the case of the correct motor operation (Figure 13). A faster increase in the temperature of the motor elements resulted from the elimination of the clearance between the cooperating components. This resulted in a dry friction, which in turn led to the release of a significant amount of frictional heat flowing directly to the motor elements, resulting in a faster heating rate of the motor elements.

The temperature of the rotor increased sharply above the temperature of the oil supplying the motor in the period of about 100 s. The temperature difference between the oil and the rotor was above 10 K. This indicates a significant amount of heat generated by friction.

In the third case (c) of testing a satellite motor in which the initial temperature was  $-4^{\circ}\text{C}$ , the oil temperature was  $54^{\circ}\text{C}$ , and the rotational speed in steady-state conditions was 185 rpm, a temporary incorrect operation occurred.

Figure 16 shows that in the initial period of the start-up, there was a short-term increase in the oil pressure at the inlet to the motor related to the oil flow resistance and acceleration of the movable parts of the motor. A few seconds after the start-up, the oil pressure was dropping. After 20 s, the pressure started to rise again, which was possibly due to a reduction in the axial clearance between the satellites and the covers.

After equalizing the temperatures of the motor elements (satellites, rotor, body), the effective axial clearance between the cooperating elements increased, and the oil pressure

at the entrance to the motor decreased. The rotational speed (flow rate) remained at the same level from the moment of start-up.

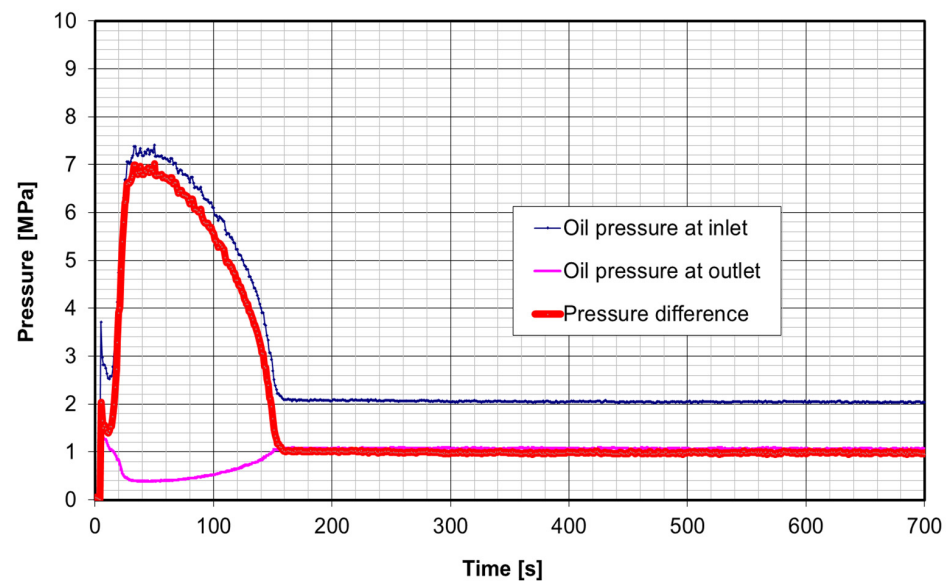


**Figure 14.** Characteristics of the oil pressure at the inlet and the outlet of the motor and their difference as a function of time (ambient temperature (motor)  $-20\text{ }^{\circ}\text{C}$ , oil temperature  $50\text{ }^{\circ}\text{C}$ , obtained rotational speed of about 255 rpm).

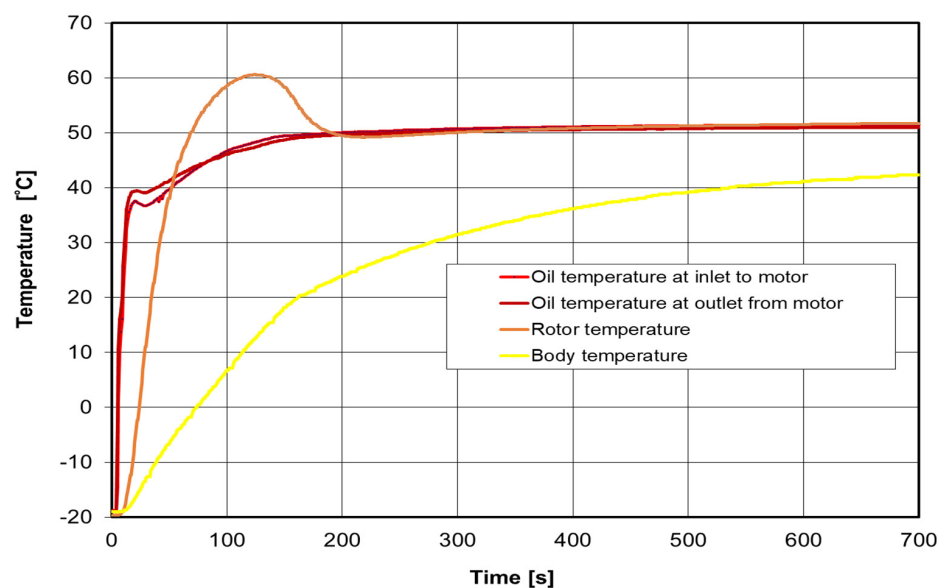


**Figure 15.** Characteristics of the temperature of rotor, body, and oil at the inlet and the outlet of the motor as a function of time (ambient temperature (motor)  $-20\text{ }^{\circ}\text{C}$ , obtained rotational speed approximately 255 rpm).

On the basis of the obtained temperature courses, it is possible to determine the temperature differences between the elements and between the oil and rotor or body. Figure 17 shows the courses of oil temperatures at the inlet and the outlet of the motor, body, and rotor as a function of time. The rotor temperature changes dynamically in the initial period. One hundred seconds after start-up, the rotor temperature was approximately 6 K lower than the oil temperature.

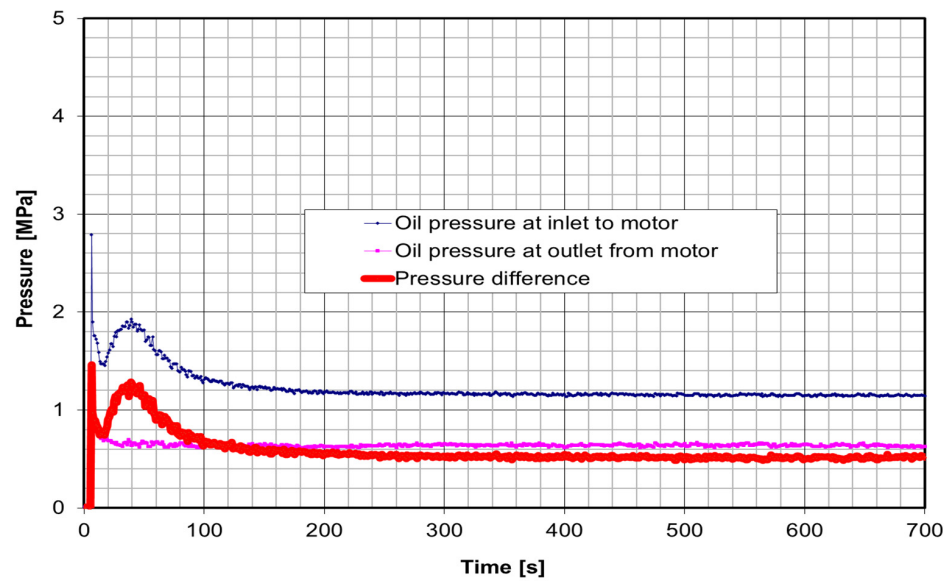


**Figure 16.** Characteristics of the oil pressure at the inlet and the outlet of the motor and the pressure difference as a function of time (ambient temperature (motor)  $-4^{\circ}\text{C}$ , oil temperature  $54^{\circ}\text{C}$ , rotational speed in steady-state conditions 185 rpm).

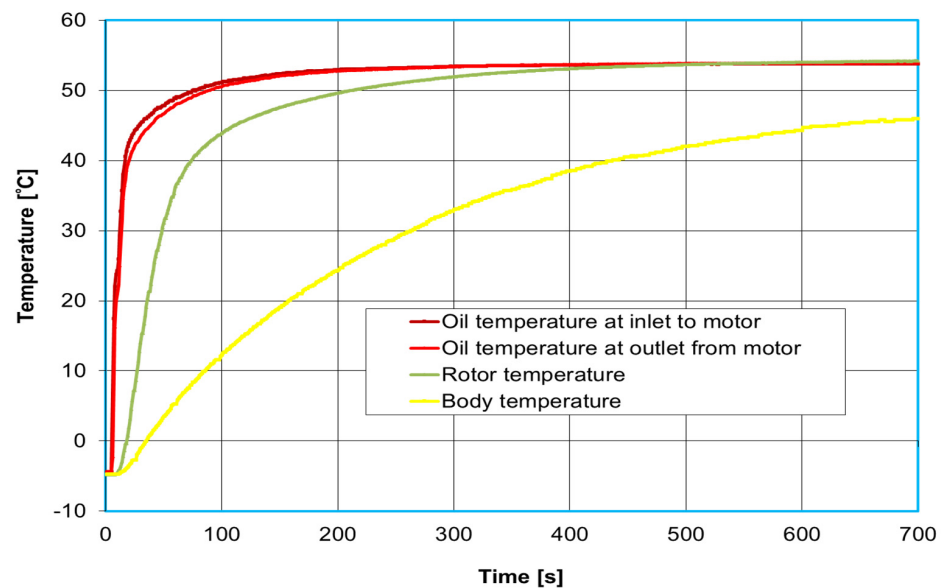


**Figure 17.** Characteristics of the temperatures of the rotor, body, and oil at the inlet and the outlet of the motor as a function of time (ambient temperature (motor)  $-4^{\circ}\text{C}$ , rotational speed in steady-state conditions 185 rpm).

## 7. Modeling of the Heating Process of the Motor Elements with the Use of Computer Simulation

The motor model was constructed and then divided into finite elements. Constraints and thermal loads have been defined.

For the computer simulation, the following should be taken into account: the initial motor (ambient) and oil temperature, as well as the heat transfer coefficients from the oil to the surface of the movable and fixed parts.

In order to illustrate the heating process of the satellite motor during start-up in thermal shock conditions, one computer simulation was carried out for the same parameters as during the experimental test in the third case (c) presented in Section 6. During this test, the conditions were as follows: initial temperature of motor (ambient temperature)  $-4^{\circ}\text{C}$ ;



temperature of the oil flowing through the motor 54 °C, rotational speed in the steady-state conditions 185 rpm. The computer simulation was carried out for these parameters (185 rpm), because the nominal rotational speed for this motor is 160 rpm.

A computer simulation in Ansys software was carried out for the following parameters: heat transfer coefficient from oil to fixed elements 1350 W/m<sup>2</sup>K, heat transfer from oil to movable parts (rotor, satellites) 900 W/m<sup>2</sup>K, heat transfer coefficient from the external surface of the motor to the environment 12 W/m<sup>2</sup>K, the initial temperature of the motor −4 °C, temperature of the oil flowing through the motor 54 °C. The heat transfer coefficients from the oil to the motor elements were determined on the basis of the results of experimental tests (element temperature courses).

A computer simulation of the heating of the motor components over time was carried out (Figure 18). The visualizations of the temperature distribution in the motor elements at 5, 10, 20, 40, 80, 160, 320, and 500 s after the warm oil was supplied to the cold motor made it possible to evaluate and analyze the heating process of the elements and individual nodes.

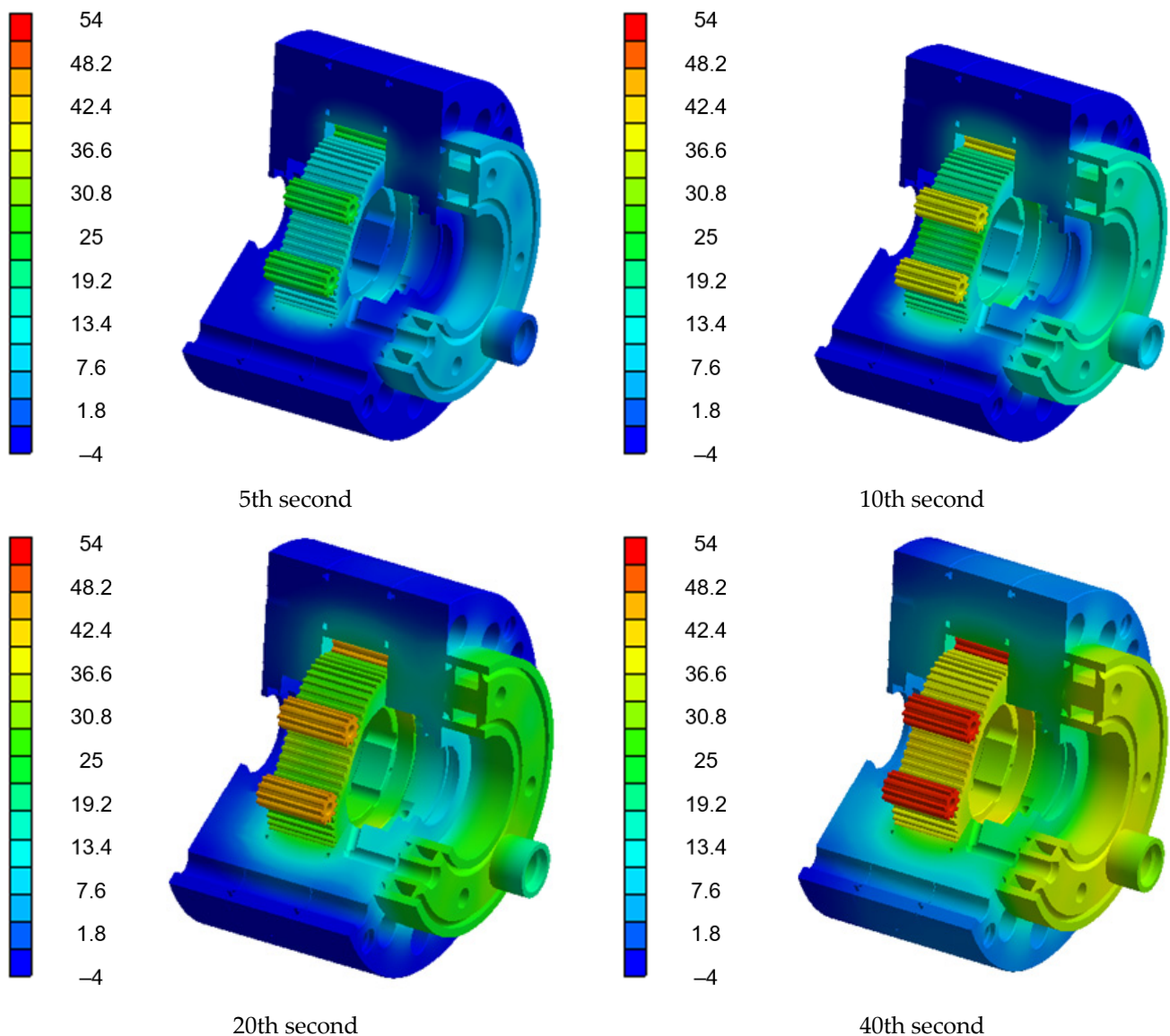
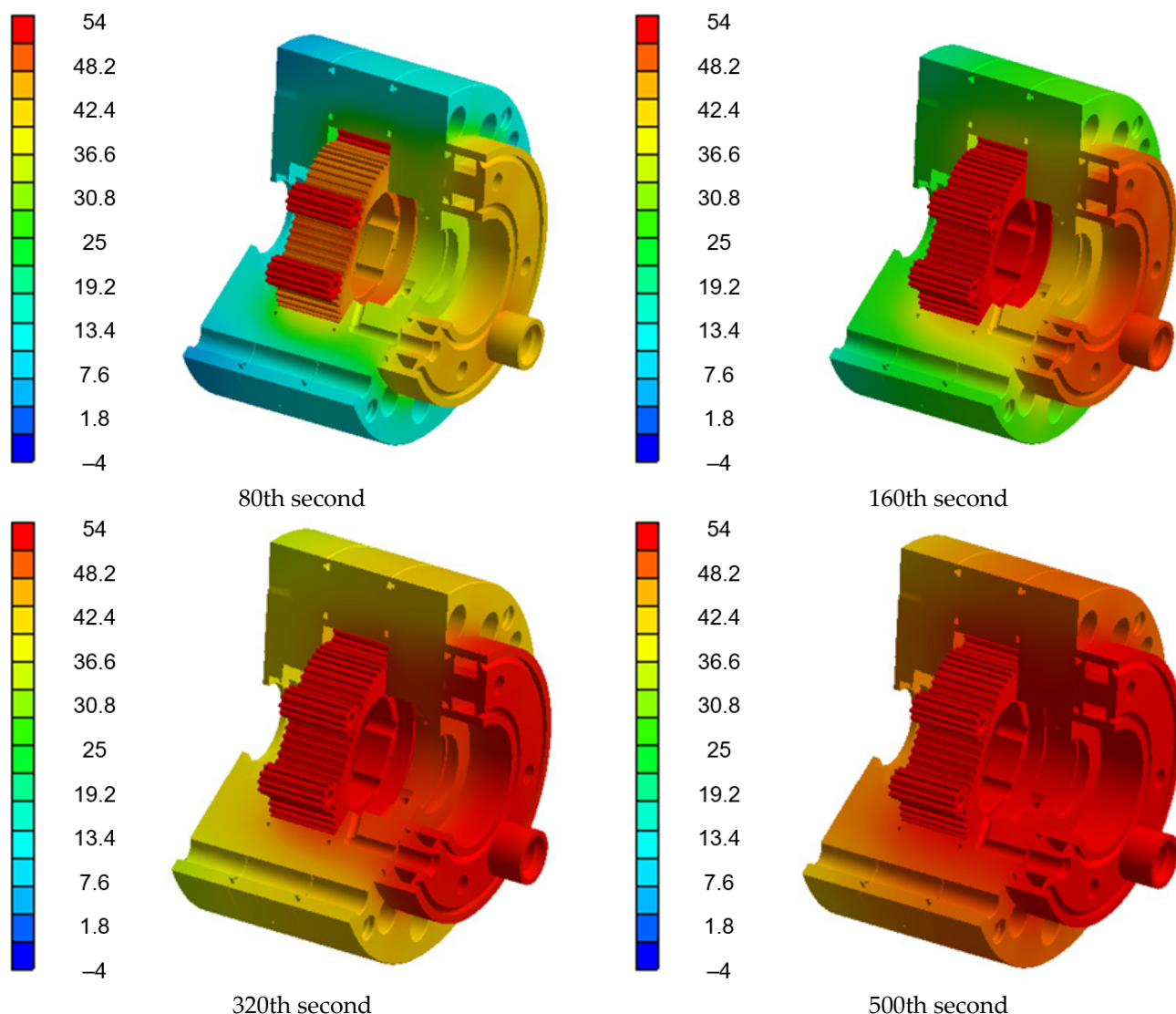


Figure 18. Cont.



**Figure 18.** Temperature distribution in warmed-up elements of M1 satellite motor (initial motor temperature  $-4\text{ }^{\circ}\text{C}$ , rotational speed in the steady-state conditions 185 rpm) at the 5th, 10th, 20th, 40th, 80th, 160th, 320th, and 500th second after supplying with  $54\text{ }^{\circ}\text{C}$  warm oil.

Satellites heat up the fastest due to their low mass and large heat transfer surface. The rotor and the supply collector heat up slightly more slowly. The slowest heat up occurs in the cover that has the least contact with the flowing warm oil and absorbs heat from more heated elements.

Using computer simulation, the temperature curves were obtained in the areas where the sensors were placed in the tested motor.

Figure 19 shows a comparison of the body temperature courses close to the heat source obtained from the experimental tests and computer simulations. In the initial period of up to 100 s, there is a very high convergence of the waveforms. Thereafter, the discrepancy is no greater than 3 K. This temperature difference between the temperature courses of the body close to the heat source obtained from the experimental tests and computer simulation may result from the fact that the same value of the heat transfer coefficient from oil to fixed elements was adopted for the computer simulation. This coefficient was determined taking into account all the fixed elements of the motor on the basis of experimental tests of the motor started in thermal shock conditions. During the experimental tests, the motor was attached to the test stand mounting plate, which was not taken into account during the

computer simulation (in the experimental tests additional elements were used to minimize the heat flow between the plate and the motor).

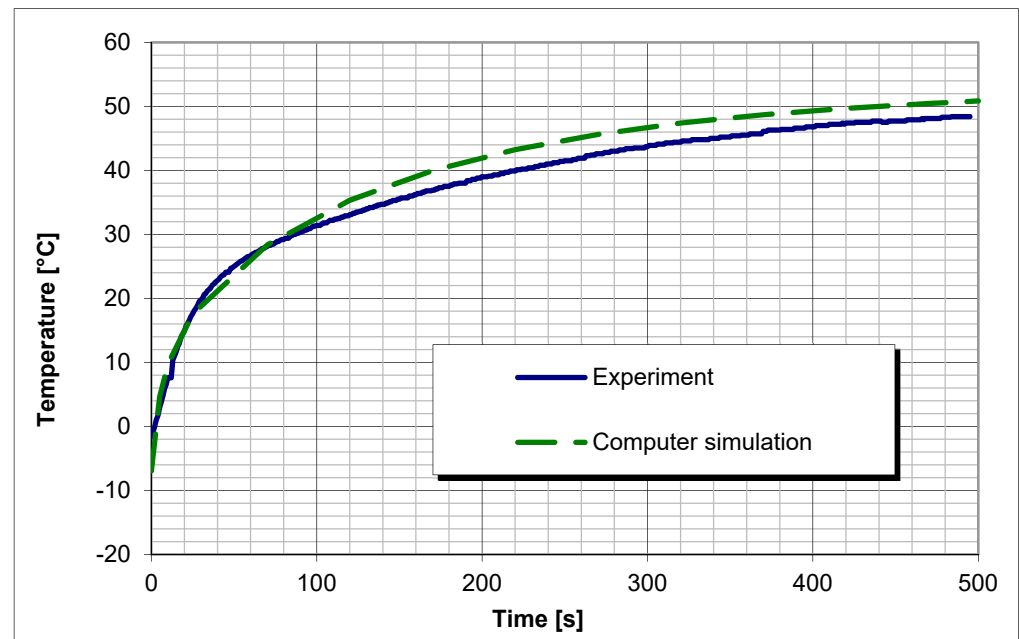


**Figure 19.** Temperature changes in the motor body close to heat source during start-up of M1 satellite motor obtained from the experimental test and computer simulation (initial motor temperature  $-4^{\circ}\text{C}$ , oil temperature  $54^{\circ}\text{C}$ , rotational speed in steady-state conditions 185 rpm).

The rotor temperature obtained from the computer simulation is slightly higher than the temperature obtained from the experimental tests (Figure 20). This is due to the fact that the heat transfer occurs from the rotor to the shaft, which was not taken into account in the computer simulation.

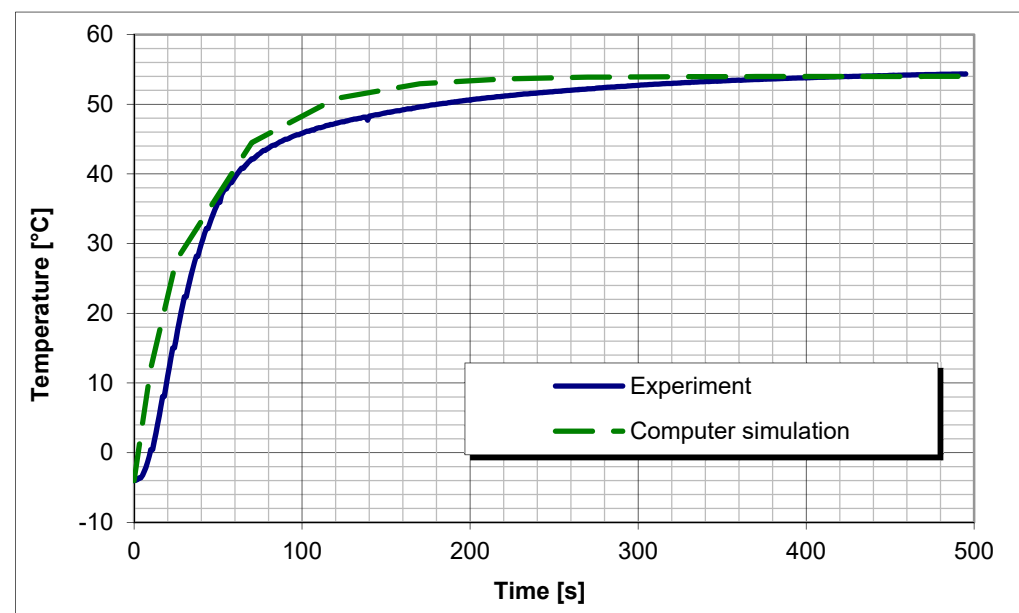


**Figure 20.** Temperature changes in the rotor during start-up of the M1 satellite motor obtained from an experimental test and computer simulation (initial motor temperature  $-4^{\circ}\text{C}$ , oil temperature  $54^{\circ}\text{C}$ , rotational speed in the steady-state conditions 185 rpm).

The temperature changes very quickly during the satellite's heating process. This is due to the large heat transfer area. The waveforms obtained from the computer simulation and experimental tests are convergent (Figure 21).

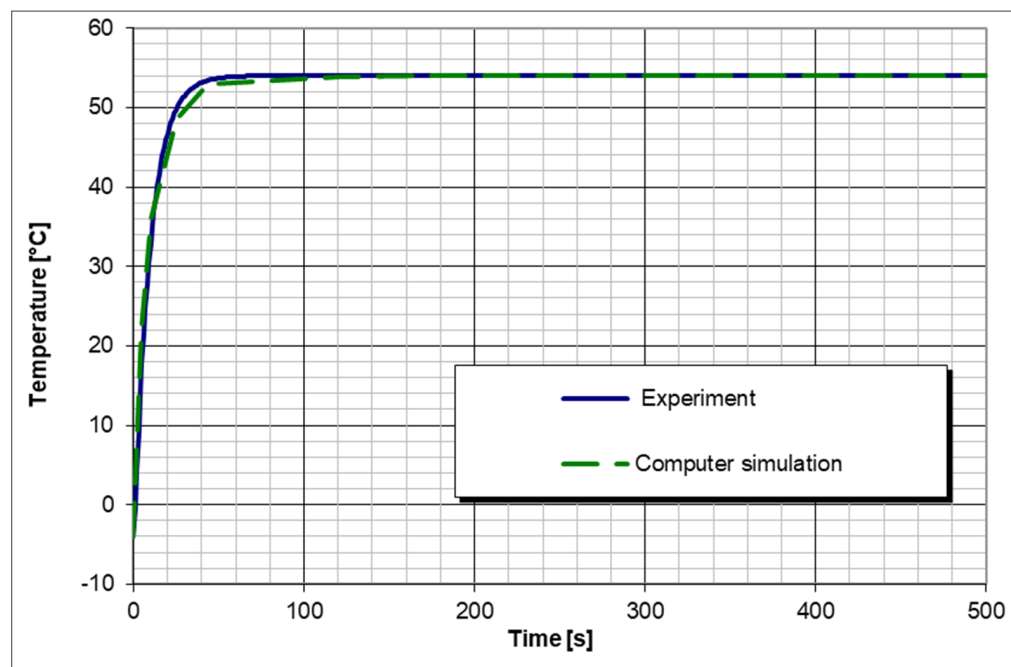


**Figure 21.** Temperature changes in the satellite during start-up of M1 satellite motor obtained from experimental test (model research) and computer simulation (initial motor temperature  $-4^{\circ}\text{C}$ , oil temperature  $54^{\circ}\text{C}$ , rotational speed in steady-state conditions 185 rpm).

With the aid of the computer simulation method, it is possible to accurately determine the heating process and obtain the temperature fields distribution of motor elements running in thermal shock conditions. Additionally, it is possible to select characteristic places in the motor where the temperature courses over time can be determined. The accuracy of the computer simulation method is shown in Figures 19–21.

The computer simulation method applied to determine the temperature fields distribution of the heated motor taking other parameters into the account is also credible. There is a high accuracy of the results from the computer simulation because, first of all, the heat transfer coefficients from the oil to the motor elements were determined on the basis of the results of experimental tests (element temperature courses), and the motor model was correctly made.

## 8. Conclusions

The developed model and method of testing hydraulic motors in thermal shock conditions enabled the analysis of the heating processes affecting moving and fixed elements of the motor. This required the design and construction of a specialized stand for testing hydraulic motors, including satellite motors, in thermal shock conditions. The stand was equipped with apparatus and a system for measuring the temperature of fixed and moving parts of the satellite motor.

Furthermore, an analysis of the influence of the friction heat in the unloaded motor on the oil temperature increase was conducted. The pressure drop in the internal channels of the motor caused by the flow resistance of the working medium and the viscous friction in the gaps of the cooperating elements cause the increase in the internal energy of the oil (increase in the oil temperature). As Figure 8 shows, with the pressure difference between the input and the output equal to 1 MPa for the unloaded satellite motor working in the steady-state conditions, the oil temperature at the output will increase by about

0.43 K. Therefore, it can be stated that frictional power losses do not significantly affect the heat exchange inside the unloaded (correctly operating) motor during start-up in thermal shock conditions.

A method for determining the correct operation of motors was developed on the basis of the example of a satellite motor, using changes in the measured parameters: pressure at the inlet to the motor and temperature of the motor elements. The temperature difference between the warm oil and the cold motor and rotational speed affects the heating process of the motor in thermal shock conditions. Starting the unloaded motor with 23  $\mu\text{m}$  axial clearance in thermal shock conditions (Figure 11) when the temperature difference between the warm oil and the cold motor does not exceed 55 K and the motor rotational speed does not exceed 250 rpm should result in the correct operation of the motor.

The author used the computer simulation method to determine the temperature fields distribution of the heated motor, assuming the heat transfer coefficient from the external surface to the environment, as well as the heat transfer coefficients from oil to the movable and fixed elements determined on the basis of experimental tests, the temperature of the working medium, and the temperature of the motor elements. The temperature courses of the body, rotor, and satellite obtained from the computer simulation are consistent with the temperature courses yielded by the experimental tests. The results of the experimental tests and computer simulations can be used to determine the heating processes of the motor elements and, also, to assess the operating conditions of the motor and to determine the extent to which they affect the possible risks of malfunction or even equipment failure.

The next step in the author's scientific activity includes the research and analysis of the heating process of the hydraulic system with a proportional valve operated in thermal shock conditions.

**Funding:** This research received no external funding.

**Institutional Review Board Statement:** Not applicable.

**Informed Consent Statement:** Not applicable.

**Conflicts of Interest:** The author declares no conflict of interest.

## References

1. Jasiński, R. Problems of the Starting and Operating of Hydraulic Units and Systems in Low Ambient Temperature (Part I). *Pol. Marit. Res.* **2008**, *15*, 37–44. [[CrossRef](#)]
2. Jasiński, R. *Badania i Metoda do Oceny Działania Zespołów Napędów Hydraulicznych Uruchamianych w Niskich Temperaturach Otoczenia Zasilanych Gorącym Czynnikiem Roboczym. (Research and Method for Assessment of Operation of Hydraulic Drive Components Started in Low Ambient Temperature and Supplied with Warm Working Medium (in Polish)). Sprawozdanie z Prac Projektu Badawczego Finansowanego Przez Ministerstwo Nauki i Szkolnictwa Wyższego, No. 4 T07C042 30; Gdańsk, Poland, 2010.*
3. Jasiński, R. *Funkcjonowanie Zespołów Napędu Hydraulicznego Maszyn w Niskich Temperaturach Otoczenia (Operation of Components of Hydraulic Drive of Machines in Low Ambient Temperatures), Monograph 166; Gdańsk University of Technology: Gdańsk, Poland, 2018.*
4. Jasiński, R. *Działanie Wybranych Wolnoobrotowych Silników Hydraulicznych w Warunkach Szoku Termicznego (Operation of Selected Low-Speed Hydraulic Motors in Thermal Shock Conditions). Ph.D. Thesis, Gdańsk University of Technology, Gdańsk, Poland, 2002.*
5. Polish Standard: PN–86/M-73079. *Ogólne Warunki Użytkowania Jednolitego Systemu Hydrauliki; Polish Committee for Standardization. Available online: [http://www.ydylstandards.org.cn/static/download/pdf/PN%20M73079-1986\\_0000.pdf](http://www.ydylstandards.org.cn/static/download/pdf/PN%20M73079-1986_0000.pdf) (accessed on 15 September 2021).*
6. Polish Committee for Standardization. *Próby Środowiskowe Wyposażenia Statków (Environmental Tests of Marine Equipment); Polski Rejestr Statków: Gdańsk, Poland, 1975.*
7. *The Rules. Environmental Tests of Marine Equipment; Publication No. 11P; Polski Rejestr Statków: Gdańsk, Poland, 1994.*
8. Balawender, A. *Analiza Energetyczna i Metodyka Badań Silników Hydraulicznych Wolnoobrotowych (Energy Analysis and Methodology for Research Low-Speed Hydraulic Motors); Zeszyty naukowe PG (Scientific Notebooks of the Gdańsk University of Technology): Gdańsk, Poland, 1988.*
9. Przychodzień, T.; Tabak, A. *Badania Silników Hydraulicznych w Obniżonych Temperaturach. Sterowanie i Napęd Hydrauliczny; Wydawnictwa Komunikacji i Łączności: Warsaw, Poland, 1981; pp. 12–15, No.1.*
10. Przychodzień, T.; Biały, J.; Dąbrowski, H.; Kulkowski, W.; Pięta, J.; Tabak, H. *Eksploracja Maszyn Roboczych w Warunkach Zimowych (Operation of Heavy Work Machines in Winter Conditions); WNT: Warszawa, Poland, 1990. (In Polish)*

11. Murrenhoff, H.; Gels, S.; Zahn, A.; Pařolat, O. Tieftemperaturuntersuchung von Zahnradpumpen. *Olhydraul. Und Pneum.* **2012**, *56*, 10–19.
12. Minav, T.; Heikkinen, J.; Schimmel, T.; Pietola, M. Direct Driven Hydraulic Drive: Effect of Oil on Efficiency in Sub-Zero Conditions. *Energies* **2019**, *12*, 219. [[CrossRef](#)]
13. Patrosz, P. Influence of Properties of Hydraulic Fluid on Pressure Peaks in Axial Piston Pumps' Chambers. *Energies* **2021**, *14*, 3764. [[CrossRef](#)]
14. Cichocki, W.; Michałowski, S.; Pobędza, J. *Badania Maszyn Roboczych i Obiektów Inżynieryjnych w Warunkach Narazeń Środowiskowych*; Wydawnictwo Politechniki Krakowskiej: Kraków, Poland, 2015.
15. *Hydraulic Motors for Drive Hydraulics (RE 00 195)*; Catalogue; Mannesmann Rexroth Group, Brueninghaus Hydromatik GmbH: Düsseldorf, Germany, 2015.
16. Zakłady Urzędzeń Okrętowych Hydroster. Silniki Hydrauliczne SOK 1 (SOK 1 Hydraulic Motors). In *Dokumentacja Techniczno-Informacyjna*; Zakłady Urzędzeń Okrętowych Hydroster: Gdańsk, Poland, 1996.
17. *Pumps and Motors*; Catalogue HY02-8001/UK; Parker Hannifin Corporation; Hydraulics Group; Tachbrook Park Drive: Warwick, UK, 2014.
18. Milecki, A.; Ortmann, J. Influences of Control Parameters on Reduction of Energy Losses in Electrohydraulic Valve with Stepping Motors. *Energies* **2021**, *14*, 6114. [[CrossRef](#)]
19. Dalla Lana, E.; De Negri, V.J. A New Evaluation Method for Hydraulic Gear Pump Efficiency through Temperature Measurements; SAE 2006 Commercial Vehicle Engineering Congress & Exhibition, Chicago, USA, 2006. Available online: [https://www.researchgate.net/publication/291083519\\_A\\_New\\_Evaluation\\_Method\\_for\\_Hydraulic\\_Gear\\_Pump\\_Efficiency\\_through\\_Temperature\\_Measurements](https://www.researchgate.net/publication/291083519_A_New_Evaluation_Method_for_Hydraulic_Gear_Pump_Efficiency_through_Temperature_Measurements) (accessed on 15 September 2021).
20. Sliwinski, P. The Methodology of Design of Axial Clearances Compensation Unit in Hydraulic Satellite Displacement Machine and Their Experimental Verification. *Arch. Civ. Mech. Eng.* **2019**, *19*, 1163–1182. [[CrossRef](#)]
21. Sliwinski, P. Determination of the Theoretical and Actual Working Volume of a Hydraulic Motor. *Energies* **2020**, *13*, 5933. [[CrossRef](#)]
22. Sliwinski, P.; Patrosz, P. Methods of Determining Pressure Drop in Internal Channels of a Hydraulic Motor. *Energies* **2021**, *14*, 5669. [[CrossRef](#)]
23. Patrosz, P. Influence of Gaps' Geometry Change on Leakage Flow in Axial Piston Pumps. In *Advances in Hydraulic and Pneumatic Drives and Control 2020*; Stryczek, J., Warzyńska, U., Eds.; Lecture Notes in Mechanical Engineering; Springer International Publishing: Cham, Switzerland, 2021; pp. 76–89. ISBN 978-3-030-59508-1.
24. Lisowski, E.; Filo, G.; Rajda, J. Analysis of the Energy Efficiency Improvement in a Load-Sensing Hydraulic System Built on the ISO Plate. *Energies* **2021**, *14*, 6735. [[CrossRef](#)]
25. Jasiński, R. Problems of the Starting and Operating of Hydraulic Components and Systems in Low Ambient Temperature: Part II Determining the Clearance between Cooperating Elements during the Hydraulic Components Start-up in Extremely Low Ambient Temperatures on the Grounds of Experimental Research. *Pol. Marit. Res.* **2009**, *15*, 61–72. [[CrossRef](#)]
26. Jasiński, R. Problems of the Starting and Operating of Hydraulic Components and Systems in Low Ambient Temperature (Part III). *Pol. Marit. Res.* **2009**, *16*, 22–31. [[CrossRef](#)]
27. Jasiński, R. Problems of the Starting and Operating of Hydraulic Components and Systems in Low Ambient Temperature (Part IV): Modelling the Heating Process and Determining the Serviceability of Hydraulic Components during the Starting-up in Low Ambient Temperature. *Pol. Marit. Res.* **2017**, *24*, 45–57. [[CrossRef](#)]
28. Staniszewki, B. *Termodynamika (Thermodynamics)*; WNT: Warszawa, Poland, 1982.
29. Hobler, T. *Ruch Ciepła i Wymienniki (Heat Transfer and Heat Exchangers)*; WNT: Warszawa, Poland, 1979.
30. Wiśniewski Stefan i Tomasz. *Wymiana Ciepła (Heat Exchange)*; Wydawnictwo Naukowo-Techniczne: Warszawa, Poland, 2000.
31. Szargut, J.; Bialecki, R.; Fic, A.; Kurpisz, K.; Nowak, A.; Rudnicki, Z.; Skorek, J. *Modelowanie Numeryczne Pól Temperatury (Numerical Modeling of Temperature Fields)*; Wydawnictwo Naukowo-Techniczne: Warszawa, Poland, 1992.
32. Szargut, J. *Termodynamika (Thermodynamics)*; Państwowe Wydawnictwo Naukowe: Warszawa, Poland, 1985.
33. Balawender, A.; Bieńkowski, A.; Barski, J. *Sprawozdanie z Badań Silników Hydraulicznych SOK-63 i SOK-100 (Report on Tests of Hydraulic Motors SOK-63 and SOK-100)*; Gdańsk, Poland, 1980.